Published in final edited form as:
J Orthop Res. 2012 January ; 30(1): 103–111. doi:10.1002/jor.21489.

Migration Responses of Outer and Inner Meniscus Cells to Applied Direct Current Electric Fields

Najmuddin J. Gunja, **Divya Dujari**, **Andrew Chen**, **Alba Luengo**, **Jason V. Fong**, and **Clark T. Hung**
Department of Biomedical Engineering, Columbia University, 351 Engineering Terrace, Mail Code 8904, 1210 Amsterdam Avenue, New York, New York 10027

Abstract

Injuries to the inner regions of the knee meniscus do not heal and can result in degenerative changes to the articular surface, ultimately leading to osteoarthritis. A possible stimulus to enhance meniscus healing is to use electric fields that induce galvanotaxis. In this study, a novel characterization of the effects of direct current electric fields on migration characteristics of meniscus cells was performed. Primary and passaged inner and outer meniscus cells were exposed to varying electric field strengths from 0 to 6 V/cm. Cell migration was tracked using time lapse digital photography, and cell displacement and cathodal direct velocity were quantified. Cytoskeletal staining was performed to examine actin distribution and nuclear content. Cell adhesion strength was quantified as a function of wall shear stress. Meniscus cells exhibited cathodal migration and cell elongation perpendicular to the applied electric field accompanied by actin reorganization. Outer meniscus cells migrated quicker and exhibited lower adhesion strengths when compared to inner meniscus cells. Passaged cells exhibited higher migration characteristics when compared to primary cells. Overall, this study demonstrated that electric fields can significantly enhance and direct meniscus cell migration and suggests the potential for their incorporation in strategies of meniscus repair and tissue engineering.

Keywords

direct current electric fields; meniscus repair; osteoarthritis; tissue engineering

The knee meniscus is a fibrocartilaginous semi-lunar shaped disc located on the tibial plateau. It serves several functions, including load transmission, shock absorption, and joint lubrication. Although several sub-types of cells are present in the meniscus,[1] the tissue can be divided into an outer region containing mainly fibroblast-like cells that are elongated or spindle-shaped and an inner region containing mainly chondrocyte-like cells that are rounded or spherical. Meniscus cells are responsible for maintaining homeostasis, and their metabolic activity depends on the forces exerted on the tissue. Although the origin of the different cell types is unclear, it is thought that during embryonic development the meniscus is formed by precursor cells expressing collagen type 2a and by cells that invade the joint and are not part of the anlagen.[2]

About 1 million surgeries are performed each year to repair meniscal lesions and tears.[3] The current gold standard is to leave small tears untreated and remove partial tears arthroscopically; however, this technique can lead to increased stresses on the articular

Correspondence to: Clark T. Hung (T: 212-854-6542; F: 212-854-8725; cth6@columbia.edu).

surface. Ideally, clinical practice should aim at meniscal preservation, and repair techniques using polymer-based arrows, darts, screws, staples, and other suture devices are being investigated.[4] None of these approaches, however, has achieved broad clinical acceptance as concerns of insufficient biomechanical stability and delayed or early polymer degradation are high. The potential of bioelectrical stimuli to aid in the repair process of soft tissues is largely unexplored. This is surprising since musculoskeletal tissues such as bone and muscle exhibit electrical activity during injury,[5,6] and endogenously generated electric fields are known to guide cell migration during wound healing and embryonic development.[7–9] Of particular interest are direct current (DC) electric fields that induce galvanotaxis and in some instances galvanotropism. Although these effects are cell and species dependent, most cell types move either to the cathode or the anode with only a few cell types insensitive to electric fields.[10]

Thus, DC electric fields may induce cell migration towards the site of meniscal injury or into scaffolds for tissue engineering. In this study, we performed a novel characterization of the effects of varying DC electric fields and cell passage number on the migration characteristics of inner meniscus (IM) and outer meniscus (OM) cells in vitro. We hypothesized that meniscus cells would exhibit cathodal migration and increased cell speeds at higher electric field strengths and passage numbers. We also hypothesized that OM cells would migrate quicker than IM cells and exhibit lower adhesion strengths.

METHODS

Cell Isolation

Medial menisci were harvested aseptically from 2- to 4-week-old bovine knee joints, divided into separate inner and outer regions (Fig. 1), minced, and digested separately for 16 h overnight using collagenase type V (696 units/mg). IM and OM cells were isolated and seeded in T-25 flasks at 25% confluence. The culture medium consisted of DMEM supplemented with 5% FBS, 0.5X nonessential amino acids, 1X essential amino acids, 10 mM HEPES, 10 mM sodium bicarbonate, 10 mM TES, 10 mM BES, 100 U/ml penicillin, and 100 mg/ml streptomycin. At 95% confluence, cells were lifted off the surface using trypsin/EDTA and counted.

Experimental Setup and Data Analysis for Galvanotaxis

IM and OM cells were plated at 37°C for 1 h, at a density of 50,000 cells/cm^2 in culture medium (10% FBS, 100 U/ml penicillin and 100 mg/ml streptomycin) on glass slides using removable flexiperm silicone vessels. Glass slides and silicone vessels were sterilized using 70% ethyl alcohol. Slides were placed in a custom-designed galvanotaxis chamber containing rectangular channels to allow for fluid flow.[14] Air bubbles were removed from the chamber by injecting culture medium. Two agarose-salt bridges were created by injecting 4% (w/v) molten agarose into Tygon-SE200 tubing, and agarose was allowed to gel. One end of each salt bridge was connected to the chamber; the other end was placed in a C-tube PBS. Each C-tube contained a Ag-Ag chloride wire for an electrode. Electrodes were created by incubating ends of the Ag wire in chlorine bleach for 20 min. The electrodes were connected to a Keithley 2410 1100V power source that was used to generate and control current flow.

Time-lapse digital microscopy was used to record cell movement using Metamorph software. Phase images were taken at 10 min intervals for 2 h. Cell movement was analyzed using ImageJ. Cell speed was calculated by determining the cell displacement between the initial cell position (at $t = 0$) and final cell position (at $t = 2$ h) divided by total elapsed time (i.e., 2 h). Directed velocity was calculated as the component of the cell speed directed to the

negative pole (cathode). Polar plots were created using MATLAB (syntax: polar(theta, rho)) by normalizing each cell to 0 μm, 0°, and plotting final distance and position of the cell at t = 2 h.

After electric field application, cells were stained to map orientation of actin filaments and the nuclei. Briefly, cells were fixed using 4% paraformaldehyde, permeabilized using 0.1% Triton X-100, and blocked using a blocking buffer consisting of 1% BSA in 1× PBS. Cells were stained with a primary vinculin antibody at a dilution of 1:500 followed by a TRITC conjugated Phalloidin antibody at a dilution of 1:100. Nuclei were subsequently counterstained using a DAPI counterstain at a dilution of 1:1,000. Images were viewed using fluorescence microscopy. Excitation and emission wavelengths for TRITC were 544 and 572 nm, respectively, and for DAPI were 345 and 458 nm, respectively.

Study 1—Varying Electric Field Strength

The speed and directed velocity of IM and OM cells at passage 1 were examined at field strengths of 0, 0.2, 0.8, 2, 4, and 6 V/cm corresponding to current densities of 0, 0.003, 0.012, 0.03, 0.07, and 0.1 A/cm^2, respectively. Cells (≥91) from each group were tracked from at least three independent slides to ensure repeatability. Incremental cell displacement was tracked at 0, 30, 60, 90, 100, 110, and 120 min for IM and OM groups stimulated at field strengths of 0 and 6 V/cm. Approximately 10 cells per group were used in the analysis. Cells were plated for 1 h prior to electric field stimulation for 2 h.

Study 2—Varying Passage Number

The speed and directed velocity of primary (P0) and passaged (P1, P2, and P3) IM and OM cells were examined at a field strength of 6 V/cm. Cells (≥54) from each group were tracked from at least three independent slides per group to ensure repeatability.

Adhesion Strength Measurements

IM and OM cells were plated as described above and placed in a custom designed flow chamber. Air bubbles were removed using PBS. The two entrances of the chamber were connected to the inlet of a Scilog peristaltic pump and to a beaker of PBS via tygon tubing to ensure continuous flow. Cells were subjected to step increases (0.4 cm^3/s) in laminar flow of PBS at 1 or 10 min intervals (total flow time of 10 min or 100 min) from 0 to 4 cm^3/s. The number of cells attached at each interval was recorded using GBTimelapse software and plotted as a function of wall shear stress (dyne/cm^2). Cells (≥60) from each group were tracked from at least five independent slides to ensure repeatability.

Statistical Analyses

All data are presented as mean ± standard deviation. The effects of electric fields on OM and IM cells and the effects of passage were examined using one-way ANOVA followed by Tukey's HSD test. Temporal OM and IM cell displacement was examined using one-way repeated measures ANOVA. If Mauchly's test of sphericity was violated, a Greenhouse–Geisser correction was performed followed by Tukey's HSD test. For adhesion strength measurements, Fisher's exact tests were performed. A $p < 0.05$ was considered significant for all statistical analyses.

RESULTS

Effect of Electric Field

The majority of the OM cells elongated and spread out on the glass surface over 2 h of stimulation, while IM cells exhibited a more rounded morphology. The majority of OM and

IM cells stimulated at 6 V/cm translocated towards the cathode and aligned perpendicular to the field (Fig. 1). Cells in the no-field control showed no preferred directionality or orientation. Cytoskeletal staining showed distinct preferential alignment of actin stress fibers (red) in groups exposed to electric field (Fig. 2). Cell spreading was greater in OM cells.

In general, increasing field strength resulted in enhanced cell speed and directionality towards the cathode for IM and OM cells (Figs. 3 and 4). OM cells exposed to 6 V/cm exhibited significantly higher migration speed of 15 ± 3 μm/h ($p = 0.01$) and cathodal directed velocity of 12 ± 4 μm/h ($p = 0.003$) when compared to OM cells at lower field strengths (Fig. 3). Percentage of cathodal OM and IM cell migration was quantified using polar plots with theta boundaries set at 210–330°. OM cells (>65%) at 4 and 6 V/cm exhibited cathodal migration (Fig. 5). In contrast, in the control group and at lower field strengths of 0.2, 0.8, and 2 V/cm, only 30–40% of OM cells exhibited cathodal migration (Fig. 5). IM cells exposed to 6 V/cm exhibited significantly higher migration speed of 9 ± 2 μm/h ($p = 0.003$) and cathodal directed velocity of 7 ± 2 μm/h ($p = 0.0002$) when compared to IM cells at lower field strengths (Fig. 4). IM cells (~60–90%) at 2, 4, and 6 V/cm exhibited cathodal migration. In contrast, in the control group and at lower field strengths of 0.2 and 0.8 V/cm, only 30–40% of IM cells exhibited cathodal migration (Fig. 6).

OM cells showed quicker cell migration trends than IM cells at each field strength including the no field controls, with significant differences observed at 2 V/cm ($p = 0.01$), 4 V/cm ($p = 0.002$), and 6 V/cm ($p < 0.0001$). OM cells exhibited significantly higher cathodal directed velocity than IM cells at 4 V/cm ($p = 0.004$) and 6 V/cm ($p < 0.0001$). A temporal examination of OM and IM cell displacement (0 and 6 V/cm) at 30 min intervals showed a linear increase in IM and OM cell displacement, albeit at different rates (Fig. 7). Significant differences were only observed among time points for the electrically stimulated OM cell group. Specifically, OM cell displacement was significantly greater ($p < 0.0001$ with Greenhouse–Geisser correction) in the last 30 min of stimulation, and the distance traveled in this time period was equivalent to or greater than that traveled in the prior 90 min. This shift in cell speed at later time points was not observed in the OM control cells or the IM cells.

Effect of Passage

Migration characteristics were examined over three passages (Fig. 8) at 6 V/cm. P3 OM cells exhibited significantly higher cell migration characteristics over the primary OM cells for cell speed ($p = 0.035$) and directed velocity ($p = 0.041$), but were not significantly different from P1 and P2 OM cells. In contrast, P3 IM cells showed significantly higher cell speed ($p = 0.002$) and directed velocity ($p = 0.002$) over primary, P1 and P2 IM cells.

Adhesion Strength Measurements

Highest adhesion strength was observed in the group with IM cells exposed to step shear stresses at 1 min intervals; the lowest strength was observed in the group with OM cells exposed to step shear stresses at 10 min intervals (Fig. 9 and Table 1).

DISCUSSION

We characterized the effects of DC electric fields on meniscus cells plated in 2D culture. Primary IM and OM cells likely contain a less homogeneous cell population than passaged cells. Thus, most experiments were performed with once passaged IM and OM cells. In response to an electric field, IM and OM cells exhibited cathodal migration and cell elongation perpendicular to the applied electric field (i.e., galvanotropism) accompanied by actin reorganization. Furthermore, higher passage cells migrated quicker than cells at lower

passages. Finally, the adhesion strengths of IM cells were found to be significantly higher than that of OM cells.

Damage to the knee meniscus can lead to a poor healing response due to a limited supply of vasculature. Thus, a vicious cycle ensues in which the normal inflammatory response and clotting cascade responsible for tissue healing and repair does not occur. As such, techniques to recruit cells to the site of injury may be particularly important for these tissues, and exogenous stimuli via electric fields may provide a mode to achieve this. Meniscal allografts[11] and devitalized meniscal plugs[12] can be repopulated with cells when placed in vivo. External stimuli, such as radiofrequency waves, enhance and direct synovial migration to heal meniscal defects in rabbits.[13] Given the correct conditions, meniscus cells close to the injury site may be able to participate in self-repair. This study examined meniscus cell migration in a 2D environment to identify appropriate exogenous stimuli necessary for enhanced and directed cell migration. Cell speed and directionality were examined at electric field intensities ≤6 V/cm as prior studies with chondrocytes showed some cell death at field strengths >6 V/cm.[14] Significant increases over the controls in cell speed and directed cathodal velocity were only observed at the higher electric field strengths. Outer, fibroblast-like meniscus cells migrated more quickly than inner chondrocyte-like meniscus cells; however, distances traveled were in the range of ligament fibroblasts for the OM cells and articular chondrocytes for IM cells.[14,15] Ensuing experiments will examine meniscus cell migration in 3D within a collagen gel that would more closely mimic the native tissue.

Migration results for controls were mirrored by adhesion tests that showed IM cells exhibited higher adhesion strength than OM cells on a glass surface. This is consistent with observed cell morphology and phenotype of IM and OM cells in culture and confirms previous findings that fibroblasts migrate more quickly than chondrocytes.[15] Adhesion strengths vary based on surface chemistry, plating time, and shear application time. In our experiment, the first two were kept constant (glass surface and 1 h plating), and the time of shear application was varied. Interestingly, for IM cells, no significant differences were observed among groups until shear stresses exceeded 266 dynes/cm^2, suggesting that integrins responsible for cell-surface adhesions stabilize and make connections to the surface relatively quickly.[16] In contrast, OM cells exposed to 10 min intervals of step increases in shear stress exhibited lower adhesion strengths when compared to respective 1 min controls at shear stresses >59 dynes/cm^2. This suggests that integrins on the OM cell surface take longer to stabilize and make cell-surface connections under the influence of external fluid flow. This disparity may also be explained by intrinsic cellular differences between IM and OM cells. OM cells express MMP-2 and MMP-3 proteases that are important for matrix remodeling and may regulate integrin formation and stability.[17] IM cells express α-smooth muscle actin, an important component in formation and stability of focal adhesions on the cell surface.[18]

Meniscus cells elongated and aligned perpendicularly to applied electric fields with the majority of cells increasing their motility towards the cathode, especially at higher electric field strengths. Due to the polar nature of water and negative surface charge associated with the chamber and cell surfaces,[19,20] in these studies, a concomitant electro-osmotic flow was directed from the anode to the cathode.[20] However, the influence of these flow fields is likely minimal as cells generally align parallel to the direction of fluid flow,[21] while in our experiment perpendicular alignment was observed. The mechanisms involved during this transformation include changes at both the cellular and molecular level.[10] At the cellular level, cell elongation and alignment is achieved through stabilization of microtubules and reorganization of actin stress fibers.[22] Actin reorganization is the major driver as its inhibition disrupts migration completely, while microtubule disruption results in reduced cell speed, but does not affect cell motility.[23] At the molecular level, cytoskeletal

rearrangement is likely influenced by an influx of ions such as calcium, through voltage-gated[24] or stretch-activated channels.[25] These ions influence actin polymerization and depolymerization dynamics and myosin contractility.[10] Electric fields also redistribute and activate growth factor receptors on the cell surface.[26] Cells contain charged surface molecules on their plasma membrane that may shift during electric field application, thereby altering and perhaps polarizing the plasma membrane.[27] Cell stimulation may also result from upregulation of autocrine motility factor that is known to activate small Rho-like GTPases and subsequently induce actin fiber reorganization.[28]

The electric field experiments were performed over a 2 h period. Most studies only report cell data at the final time point; however, cell migration trends at shorter times may also be significant. We observed that OM cells traveled quickest in the last 30 min of stimulation. Acceleration in cell speed was absent in IM cells exposed to electric fields and in both IM and OM control groups where cell migration occurred at a uniform pace through the 2 h period. These findings indicate meniscus cells may require priming for longer periods to garner maximum cell displacement and directed velocity. Alternatively, other stimuli such as growth factors may be used synergistically with electric fields to enhance and direct cell migration.[29]

Passaged meniscus cells were used as they are common in tissue engineering studies where primary cells are scarce and must be expanded to attain sufficient cell numbers. Enhanced cell speed and directed cathodal velocity was observed with increasing passage number. This was not surprising as meniscus cells differentiate with passage towards a fibroblastic lineage,[30] and fibroblasts are known to migrate quicker than chondrocytes.[14,15]

Our results have direct implications for meniscus tissue engineering studies in which spatial sorting of cells within a scaffold system is important and may influence functional properties of the construct. A scaffold can be devised to include primary or passaged cells from both the IM and OM. Differences in cell migration speed between OM and IM cells may affect desired spatial cell sorting within the scaffold after electric field stimulation. This concept has been examined for fibroblast migration within a 3D-collagen gel.[31] In another study by the same group comparing fibroblasts and bone marrow-derived mesenchymal stem cells, the authors showed that fibroblasts were able to reorient the collagen matrix to a greater degree than were the mesenchymal stem cells.[32] This result is consistent with the higher adhesion strengths of the mesenchymal stem cells, which presumably allows them to resist reorientation in the field. Alternatively, surface properties of the scaffold may be modulated to achieve desired adhesion strengths required for optimal cell migration or reorientation. Thus, our study can be used as a platform for future meniscus tissue engineering studies utilizing primary or passaged meniscus cells for scaffold-based tissue engineering.

In conclusion, we demonstrated that applied electric fields can significantly enhance and direct IM and OM cell migration. To build on these results, future experiments should examine meniscus migration on ECM substrates and through dense matrices, as substrates can influence cell motility and galvanotactic response.[15,33] An examination of the effect of electric fields on co-cultures of meniscus cells and synoviocytes may also provide a more realistic picture, as synoviocytes aid in meniscus repair.[13] In addition, in vivo techniques used in other applications[34–36] to generate and quantify electric fields will need to be further developed for the meniscus repair scenario.

Acknowledgments

The authors would like to acknowledge our funding source NIH AR52871 and Keith Yeager for his help with the loading chamber.

REFERENCES

1. McDevitt CA, Mukherhee S, Kambic HE, et al. Emerging concepts of the cell biology of the meniscus. Curr Opin Orthop. 2002; 13:345–350.
2. Hyde G, Boot-Handford RP, Wallis GA. Col2a1 lineage tracing reveals that the meniscus of the knee joint has a complex cellular origin. J Anat. 2008; 213:531–538. [PubMed: 19014360]
3. Small NC. Complications in arthroscopic surgery performed by experienced arthroscopists. Arthroscopy. 1988; 4:215–221. [PubMed: 3166663]
4. Lozano J, Ma CB, Cannon WD. All-inside meniscus repair: a systematic review. Clin Orthop Relat Res. 2007; 455:134–141. [PubMed: 17179785]
5. Lokietek W, Pawluk RJ, Bassett CA. Muscle injury potentials: a source of voltage in the undeformed rabbit tibia. J Bone Joint Surg Br. 1974; 56:361–369. [PubMed: 4853297]
6. Chakkalakal DA, Wilson RF, Connolly JF. Electrophysiologic basis for prognosis in fracture-healing. Med Instrum. 1988; 22:312–322.
7. Huttenlocher A, Horwitz AR. Wound healing with electric potential. N Engl J Med. 2007; 356:303–304. [PubMed: 17229960]
8. Levin M. Bioelectromagnetics in morphogenesis. Bioelectromagnetics. 2003; 24:295–315. [PubMed: 12820288]
9. Nuccitelli R. Endogenous electric fields in embryos during development, regeneration and wound healing. Radiat Prot Dosimetry. 2003; 106:375–383. [PubMed: 14690282]
10. Mycielska ME, Djamgoz MB. Cellular mechanisms of direct-current electric field effects: galvanotaxis and metastatic disease. J Cell Sci. 2004; 117(Pt 9):1631–1639. [PubMed: 15075225]
11. Jackson DW, Simon T. Assessment of donor cell survival in fresh allografts (ligament, tendon, and meniscus) using DNA probe analysis in a goat model. Iowa Orthop J. 1993; 13:107–114. [PubMed: 7820730]
12. Kambic HE, Futani H, McDevitt CA. Cell, matrix changes and alpha-smooth muscle actin expression in repair of the canine meniscus. Wound Repair Regen. 2000; 8:554–561. [PubMed: 11208183]
13. Hatayama K, Higuchi H, Kimura M, et al. Histologic changes after meniscal repair using radiofrequency energy in rabbits. Arthroscopy. 2007; 23:299–304. [PubMed: 17349474]
14. Chao PH, Roy R, Mauck RL, et al. Chondrocyte translocation response to direct current electric fields. J Biomech Eng. 2000; 122:261–267. [PubMed: 10923294]
15. Chao PH, Lu HH, Hung CT, et al. Effects of applied DC electric field on ligament fibroblast migration and wound healing. Connect Tissue Res. 2007; 48:188–197. [PubMed: 17653975]
16. Shattil SJ, Kim C, Ginsberg MH. The final steps of integrin activation: the end game. Nat Rev Mol Cell Biol. 11:288–300. [PubMed: 20308986]
17. Davidson B, Goldberg I, Gotlieb WH, et al. Coordinated expression of integrin subunits, matrix metalloproteinases (MMP), angiogenic genes and Ets transcription factors in advanced-stage ovarian carcinoma: a possible activation pathway? Cancer Metastasis Rev. 2003; 22:103–115. [PubMed: 12716042]
18. Hinz B, Dugina V, Ballestrem C, et al. Alpha-smooth muscle actin is crucial for focal adhesion maturation in myofibroblasts. Mol Biol Cell. 2003; 14:2508–2519. [PubMed: 12808047]
19. Finkelstein EI, Chao PH, Hung CT, et al. Electric field-induced polarization of charged cell surface proteins does not determine the direction of galvanotaxis. Cell Motil Cytoskeleton. 2007; 64:833–846. [PubMed: 17685443]
20. Hung CT, Allen FD, Pollack SR, et al. What is the role of the convective current density in the real-time calcium response of cultured bone cells to fluid flow? J Biomech. 1996; 29:1403–1409. [PubMed: 8894920]
21. Ives CL, Eskin SG, McIntire LV. Mechanical effects on endothelial cell morphology: in vitro assessment. In Vitro Cell Dev Biol. 1986; 22:500–507. [PubMed: 3759792]
22. Harris AK, Pryer NK, Paydarfar D. Effects of electric fields on fibroblast contractility and cytoskeleton. J Exp Zool. 1990; 253:163–176. [PubMed: 2313246]

23. Finkelstein E, Chang W, Chao PH, et al. Roles of microtubules, cell polarity and adhesion in electric-field-mediated motility of 3T3 fibroblasts. J Cell Sci. 2004; 117(Pt 8):1533–1545. [PubMed: 15020680]
24. Cho MR, Thatte HS, Silvia MT, et al. Transmembrane calcium influx induced by ac electric fields. FASEB J. 1999; 13:677–683. [PubMed: 10094928]
25. Lee J, Ishihara A, Oxford G, et al. Regulation of cell movement is mediated by stretch-activated calcium channels. Nature. 1999; 400(6742):382–386. [PubMed: 10432119]
26. Zhao M, Pu J, Forrester JV, et al. Membrane lipids, receptors EGF intracellular signals colocalize are polarized in epithelial cells moving directionally in a physiological electric field. FASEB J. 2002; 16:857–859. [PubMed: 11967227]
27. Patel N, Poo MM. Orientation of neurite growth by extracellular electric fields. J Neurosci. 1982; 2:483–496. [PubMed: 6279799]
28. Yanagawa T, Funasaka T, Tsutsumi S, et al. Novel roles of the autocrine motility factor/phosphoglucose isomerase in tumor malignancy. Endocr Relat Cancer. 2004; 11:749–759. [PubMed: 15613449]
29. Fang KS, Farboud B, Nuccitelli R, et al. Migration of human keratinocytes in electric fields requires growth factors and extracellular calcium. Journal of Investigative Dermatology. 1998; 111:751–756. [PubMed: 9804333]
30. Gunja NJ, Athanasiou KA. Passage and reversal effects on gene expression of bovine meniscal fibrochondrocytes. Arthritis Res Ther. 2007; 9:R93. [PubMed: 17854486]
31. Sun S, Cho M. Human fibroblast migration in three-dimensional collagen gel in response to noninvasive electrical stimulus—II. Identification of electrocoupling molecular mechanisms. Tissue Engineering. 2004; 10:1558–1565. [PubMed: 15588415]
32. Sun S, Titushkin I, Cho M. Regulation of mesenchymal stem cell adhesion and orientation in 3D collagen scaffold by electrical stimulus. Bioelectrochemistry. 2006; 69:133–141. [PubMed: 16473050]
33. Helary C, Foucault-Bertaud A, Godeau G, et al. Fibroblast populated dense collagen matrices: cell migration, cell density and metalloproteinases expression. Biomaterials. 2005; 26:1533–1543. [PubMed: 15522755]
34. Otter MW, McLeod KJ, Rubin CT. Effects of electromagnetic fields in experimental fracture repair. Clin Orthop Relat Res. 1998; 355(Supp 1):S90–S104. [PubMed: 9917630]
35. Gan JC, Glazer PA. Electrical stimulation therapies for spinal fusions: current concepts. Eur Spine J. 2006; 15:1301–1311. [PubMed: 16604354]
36. Tyner KM, Kopelman R, Philbert MA. “Nanosized voltmeter’’ enables cellular-wide electric field mapping. Biophys J. 2007; 93:1163–1174. [PubMed: 17513359]

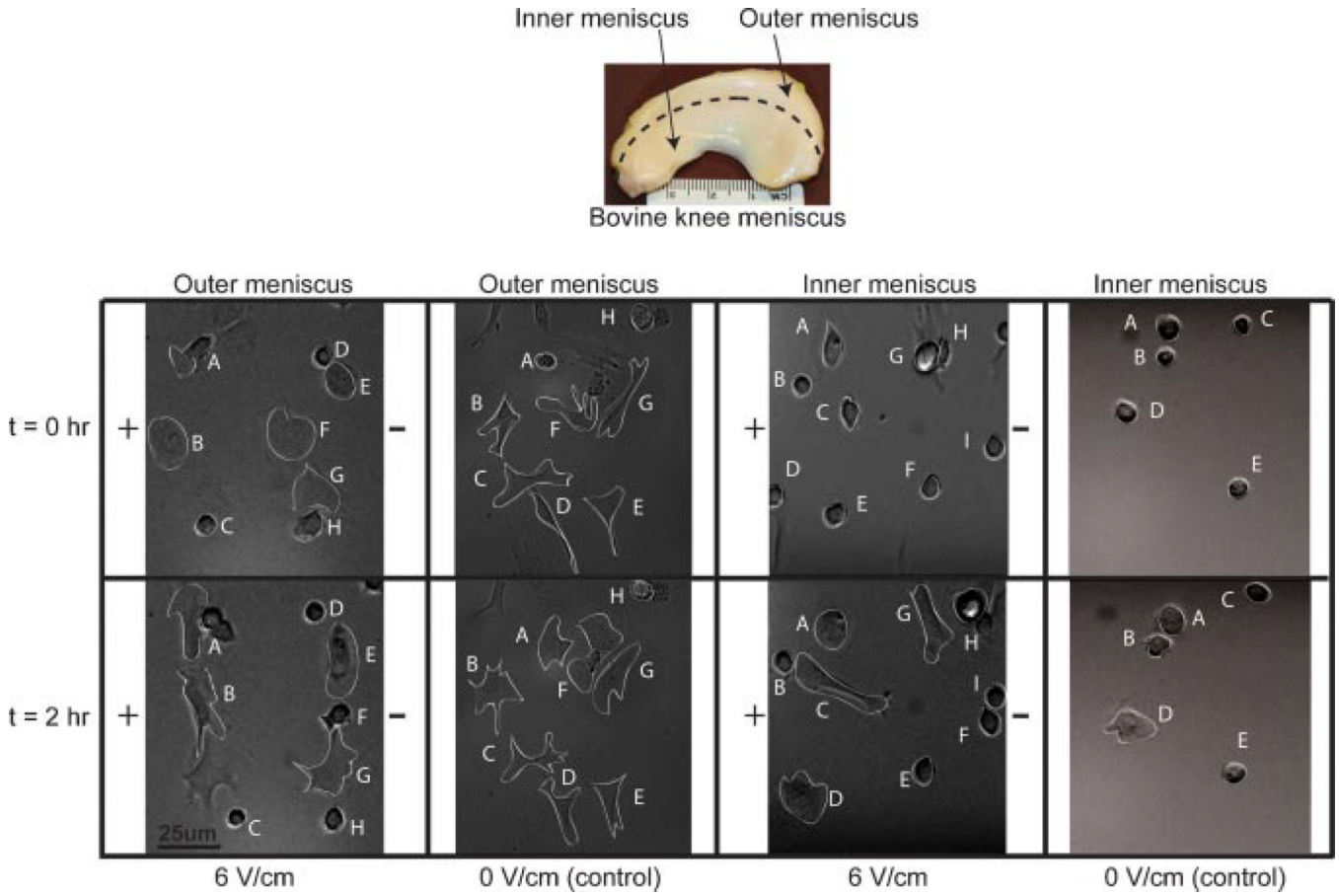

Figure 1.
Cell migration and alignment of OM and IM cells in the presence and absence of electric field. Letters track cell migration of individual cells over 2 h.

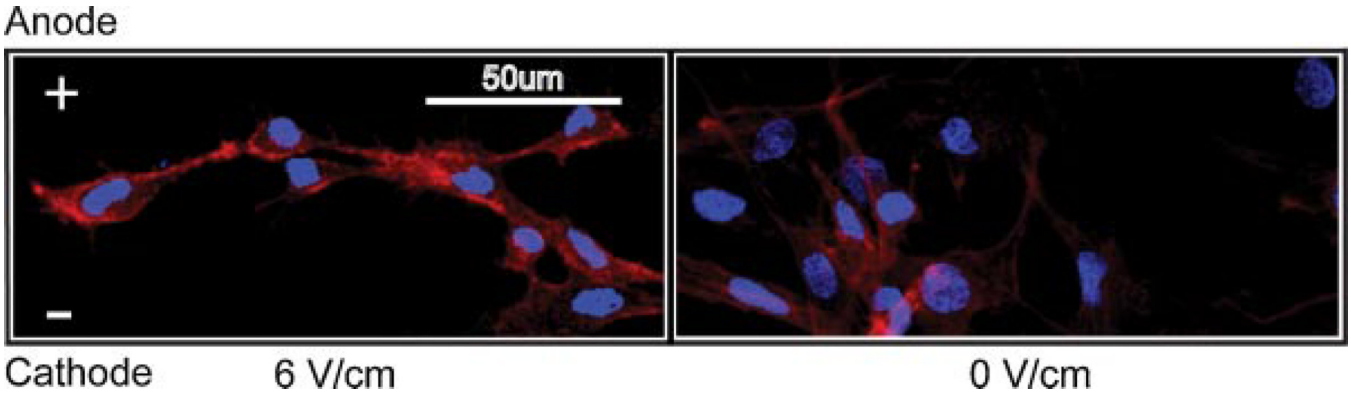

Figure 2.
Actin and nuclear staining of OM cells at 2 h post-stimulation. Nucleus is shown in blue, and actin is shown in red.

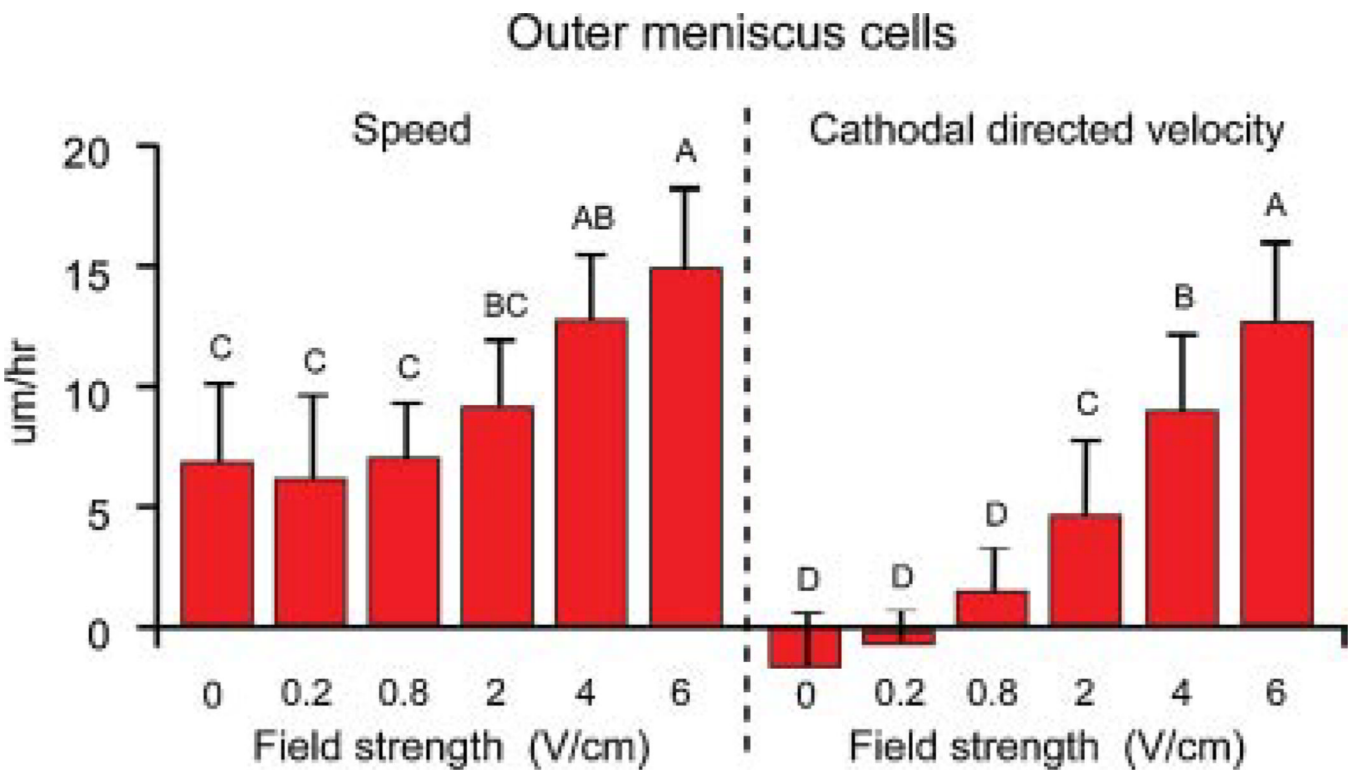

Figure 3.
Speed and cathodal directed velocity of OM cells at various electric field strengths. Groups with different letters are significantly different from each other. n = 102–174 cells from three to five slides per group.

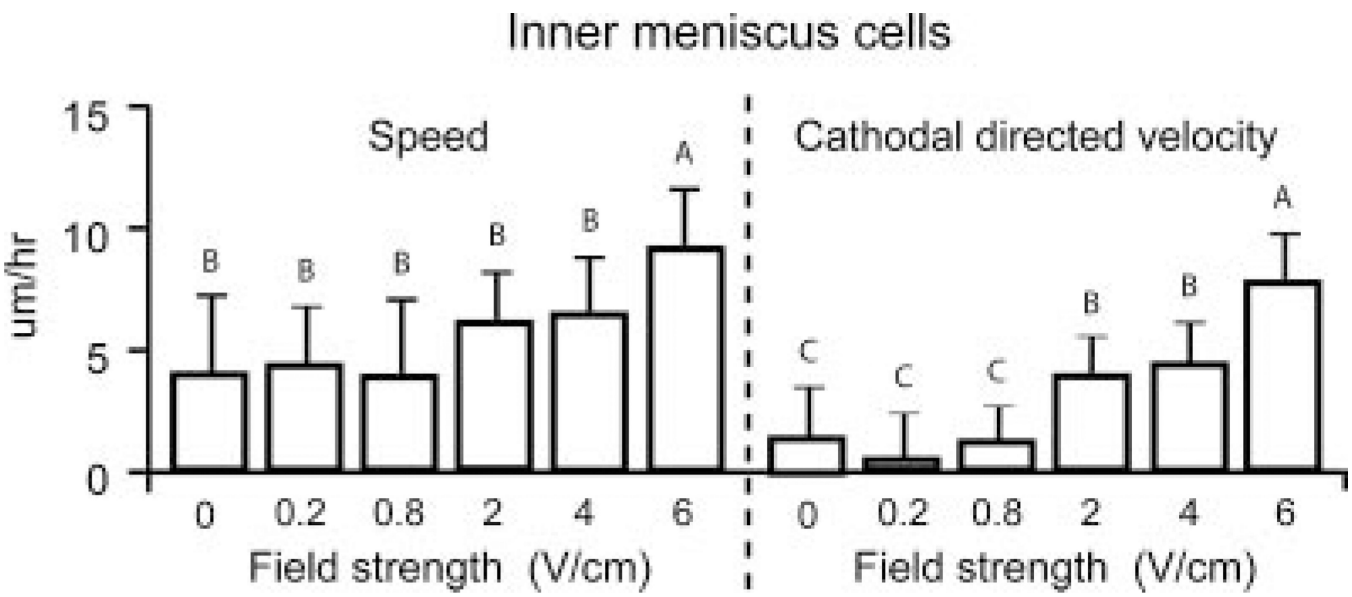

Figure 4.
Speed and cathodal directed velocity of IM cells at various electric field strengths. Groups with different letters are significantly different from each other. n = 92–144 cells from three to five slides per group.

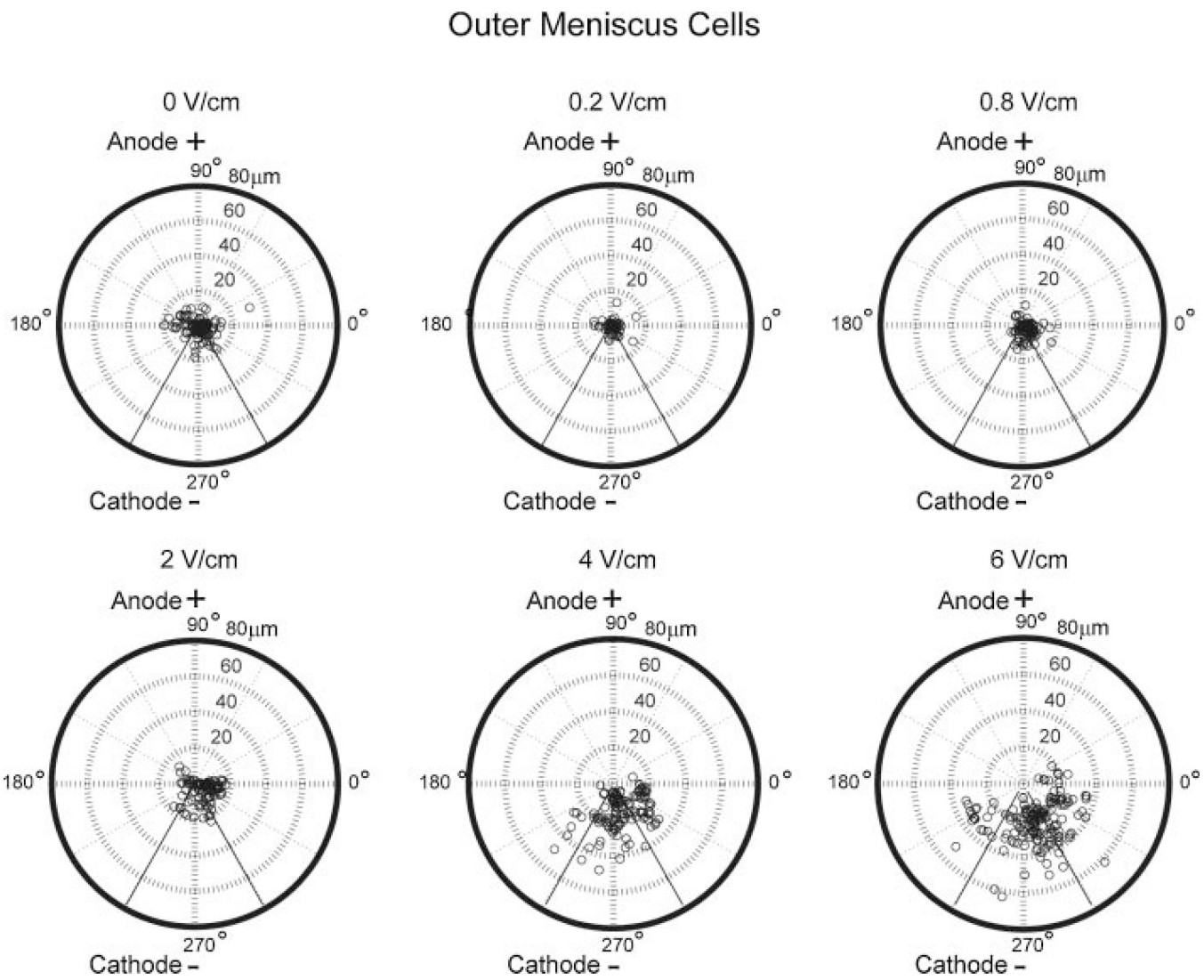

Figure 5.
Polar plots of OM cells at electric fields strengths of 0, 0.2, 0.8, 2, 4, and 6 V/cm.

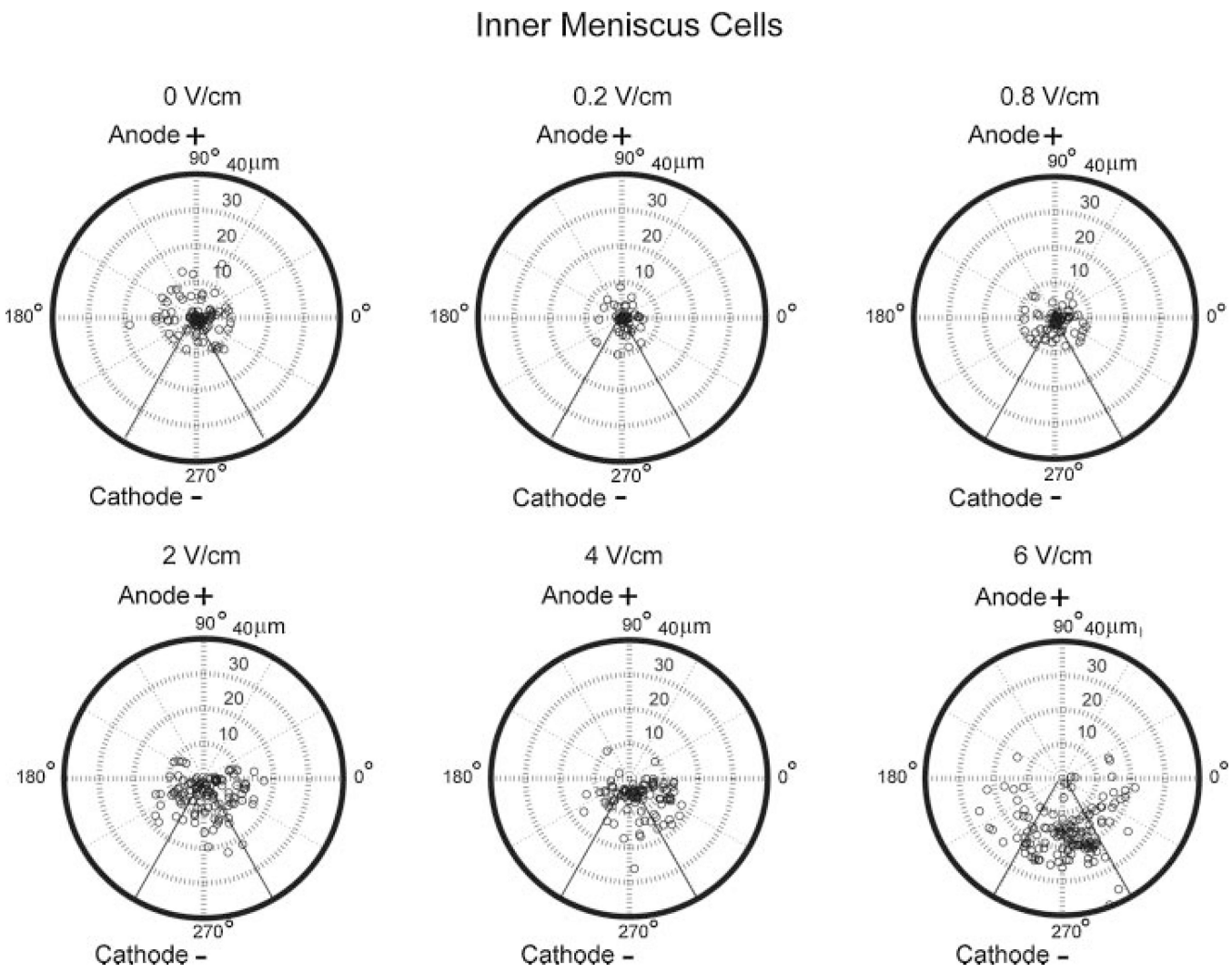

Figure 6.
Polar plots of IM cells at electric fields strengths of 0, 0.2, 0.8, 2, 4, and 6 V/cm.

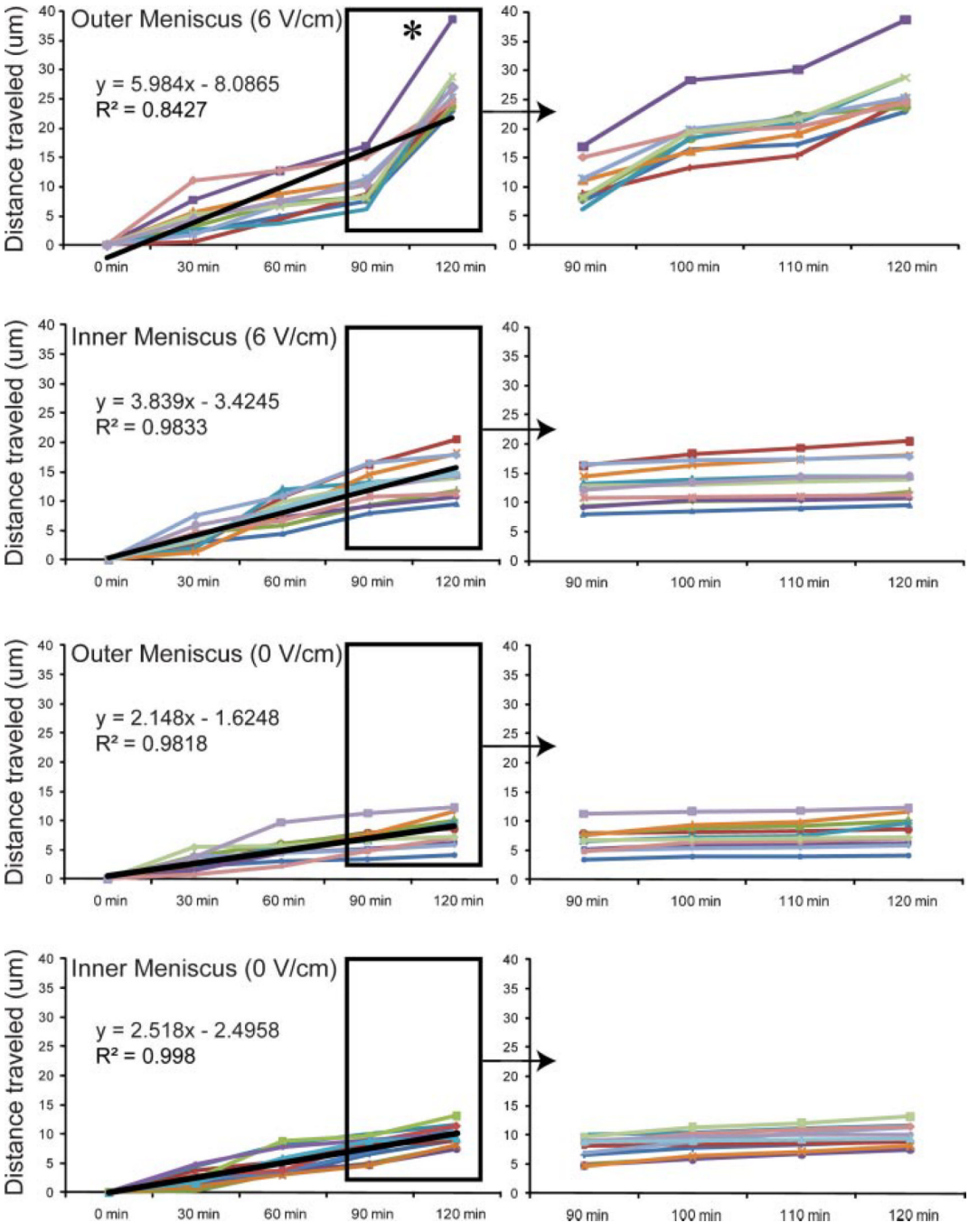

Figure 7.

Temporal IM and OM cell displacement profiles at 0 and 6 V/cm. Star symbol refers to significant difference among groups using one-way repeated measures ANOVA. $n = 9–11$ cells per group.

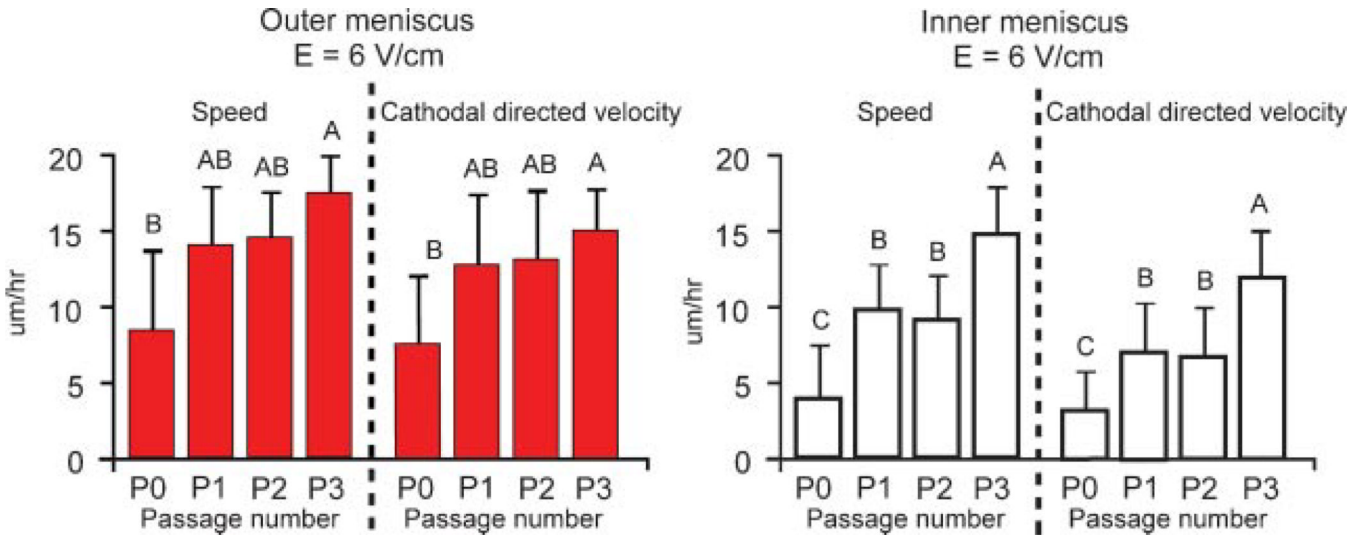

Figure 8.

Effect of passage on cell migration of OM and IM cells at 0 and 6 V/cm. n = 54–66 OM cells from three slides per passage and 55–69 IM cells from three slides per passage. Groups with different letters are significantly different from each other.

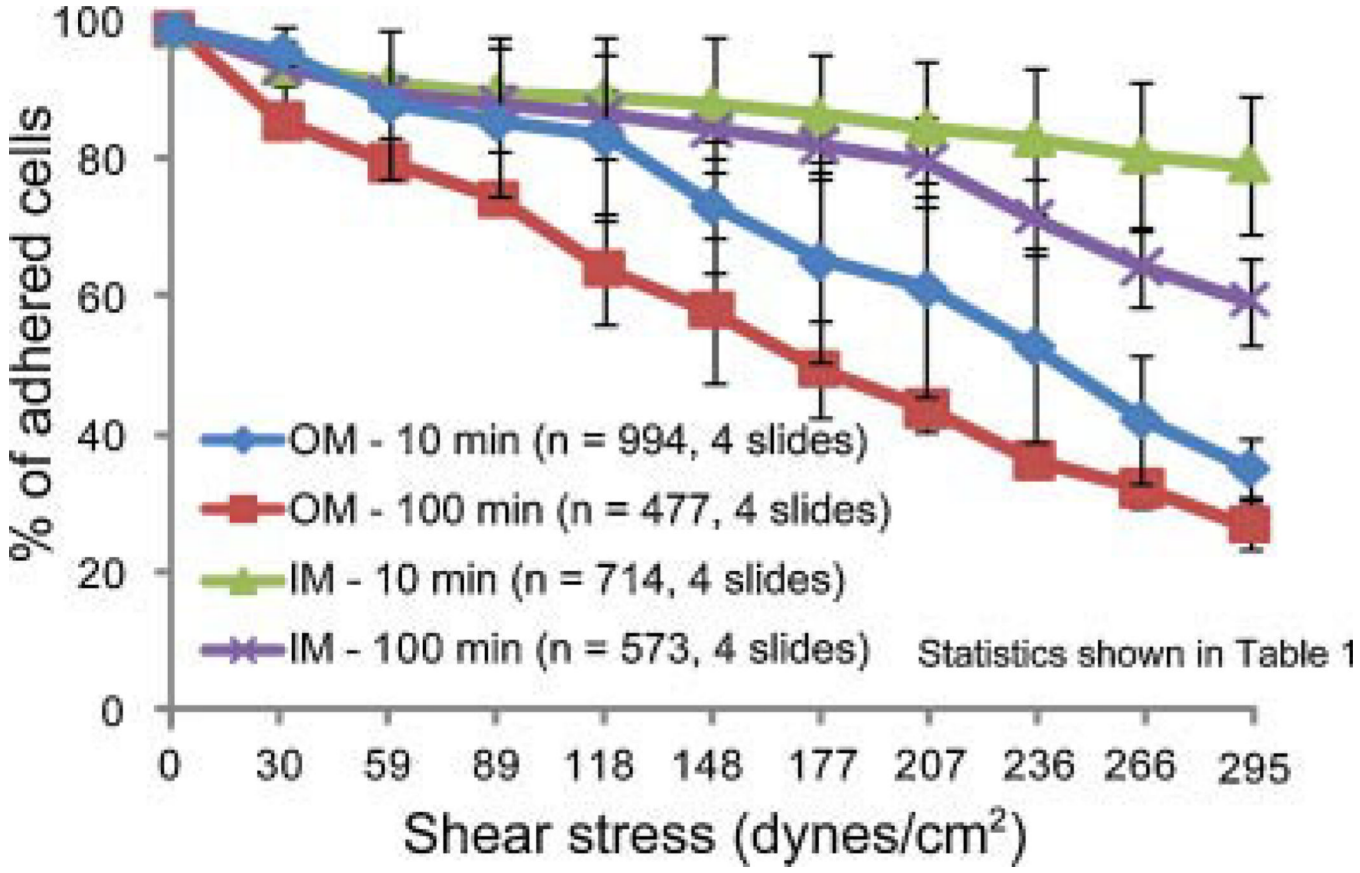

Figure 9.
Adhesion strengths of OM and IM cells with 10 and 100 min plating times.

Table 1

Statistical Differences in Adhesion Strength between IM and OM Cells

Group Comparisons	Shear Stress Values Where Significance Was Observed (dynes/cm^2)
OM (10 min) vs. OM (100 min)	≥59
IM (10 min) vs. IM (100 min)	≥266
OM (100 min) vs. IM (100 min)	≥89
OM (10 min) vs. IM (10 min)	≥177